American Journal of Transplantation 2017; 17: 1229–1241
Wiley Periodicals Inc.

doi: 10.1111/ajt.14103

Simultaneously Targeting Myofibroblast Contractility and Extracellular Matrix Cross-Linking as a Therapeutic Concept in Airway Fibrosis

Y.-C. Lin[1,2], Y. K. Sung[2], X. Jiang[1,2], M. Peters-Golden[3] and M. R. Nicolls[1,2,*]

[1]Division of Pulmonary and Critical Care Medicine, Department of Medicine, Stanford University, Stanford, CA
[2]Veterans Affairs Palo Alto Health Care System, Palo Alto, CA
[3]Division of Pulmonary and Critical Care Medicine, Department of Medicine, University of Michigan, Ann Arbor, Ann Arbor, MI
**Corresponding author: Mark R. Nicolls, mnicolls@stanford.edu*

Fibrosis after solid organ transplantation is considered an irreversible process and remains the major cause of graft dysfunction and death with limited therapies. This remodeling is characterized by aberrant accumulation of contractile myofibroblasts that deposit excessive extracellular matrix (ECM) and increase tissue stiffness. Studies demonstrate, however, that a stiff ECM itself promotes fibroblast-to-myofibroblast differentiation, stimulating further ECM production. This creates a positive feedback loop that perpetuates fibrosis. We hypothesized that simultaneously targeting myofibroblast contractility with relaxin and ECM stiffness with lysyl oxidase inhibitors could break the feedback loop, reversing established fibrosis. To test this, we used the orthotopic tracheal transplantation (OTT) mouse model, which develops robust fibrotic airway remodeling. Mice with established fibrosis were treated with saline, mono-, or combination therapies. Although monotherapies had no effect, combining these agents decreased collagen deposition and promoted re-epithelialization of remodeled airways. Relaxin inhibited myofibroblast differentiation and contraction in a matrix-stiffness–dependent manner through prostaglandin E_2 (PGE_2). Furthermore, the effect of combination therapy was lost in PGE_2 receptor knockout and PGE_2-inhibited OTT mice. This study revealed the important synergistic roles of cellular contractility and tissue stiffness in the maintenance of fibrotic tissue and suggests a new therapeutic principle for fibrosis.

Abbreviations: BAPN, β-aminopropionitrile; Cntrl, control; COX2, cyclooxygenase 2; CTCF, corrected total cell fluorescence; DAPI, 4′,6-diamidino-2-phenylindole; DMEM, Dulbecco's modified Eagle medium; ECM, extracellular matrix; EP_2, E prostanoid 2; IPF, idiopathic pulmonary fibrosis; LFA1, lymphocyte function-associated antigen 1; LGR7, leucine-rich repeat–containing G protein-coupled receptor 7; LOXL2, lysyl oxidase–like 2; LOX, lysyl oxidase; NS, not significant; OTT, orthotopic tracheal transplantation; PBS, phosphate-buffered saline; PGE_2, prostaglandin E_2; pMLC, phospho–myosin light chain; Rlxn, relaxin; RMST, root mean square tractions; RXFP1, relaxin receptor 1; SEM, standard error of the mean; α-SMA, α–smooth muscle actin

Received 06 July 2016, revised 05 October 2016 and accepted for publication 25 October 2016

Introduction

After tissue injury, the reparative response is characterized by a transient appearance of myofibroblasts that produce provisional, collagenous scars that protect against further damage and rupture. In a normal response, the provisional scars are eventually replaced by normal tissue. In fibrosis, however, accumulation and activation of myofibroblasts are persistent, resulting in overproduction of stiff extracellular matrix (ECM) that replaces the normal tissue. Because few therapeutic options exist for reversing fibrosis, this process may cause organ dysfunction and death. Previous studies have demonstrated that the increased ECM stiffness that occurs in fibrosis is not only a consequence of myofibroblast activation but also a causative factor that independently perpetuates fibrosis (1,2). The mechanical resistance of the ECM stimulates myofibroblasts to express α–smooth muscle actin (α-SMA), which enables cell contraction. This cellular conversion then triggers the secretion and activation of cytokines and growth factors, leading to additional ECM production and creating a positive feedback loop (3).

Recent antifibrotic strategies targeting myofibroblast differentiation and contraction have shown promising results (4). Among these approaches is the use of relaxin. Relaxin appears to inhibit fibrosis by attenuating cellular contraction (5,6). Despite the lack of full understanding of its mechanisms of action, relaxin was tested for the treatment of systemic sclerosis. An early placebo-controlled trial showed that low-dose relaxin significantly

reduced skin thickening and stabilized lung function (7). Subsequent phase II and III trials, however, found no significant benefit (8).

Other antifibrotic strategies have attempted to decrease tissue stiffness by targeting collagen cross-linking, the principal determinant of ECM stiffness. Lysyl oxidase (LOX) is an enzyme that catalyzes the covalent cross-linking of myofibroblast-secreted collagen units into insoluble fibers (9). LOX is upregulated in fibrosis and is associated with greater tissue stiffness in patients (10). Animal studies have shown that inhibition of LOX and LOX-like 2 (LOXL2) suppresses fibrosis in various organs (11,12); however, clinical trials of LOXL2 inhibition were terminated because of lack of efficacy.

Targeting myofibroblast contractility or ECM stiffness individually has not yet been shown to be effective for the treatment of human fibrotic disease, possibly because both components are linked through a positive feedback loop and likely require individualized drug targeting. To address this possibility, we used the orthotopic tracheal transplantation (OTT) mouse model. Rejection of OTT allografts is characterized by the destruction of the airway microvasculature and epithelial cell layer followed by an accumulation of myofibroblasts that deposit progressively cross-linked subepithelial collagen, analogous to large airway changes seen in lung transplantation (13); OTT mice do not develop bronchiolitis obliterans. Evaluating changes in OTTs permits a detailed physiologic and architectural assessment from which careful inferences can be drawn concerning the process of generalized fibrosis and fibrosis attenuation in large airways. Unlike the fibrosis in the bleomycin lung injury model, which is spontaneously reversible, the fibrosis in OTTs is persistent and unresponsive to all immunomodulating agents tested to date (14) and may model certain intractable features of chronic lung allograft dysfunction. In this study, we sought to determine whether targeting both components of the biophysical microenvironment, namely, myofibroblast contractility with relaxin and ECM stiffness with LOX inhibition, could facilitate self-repair and reduce fibrosis after "irreversible" tissue remodeling was well established.

Materials and Methods

Animals and experimental procedures

Mice were acquired from the Jackson Laboratory (Bar Harbor, ME). Animal procedures were approved by the U.S. Department of Veterans Affairs Palo Alto Health Care System institutional animal care and utilization committee. OTTs were performed as described previously (15). In short, tracheal segments from BALB/cJ (allograft) or C57BL/6J (syngraft) donor mice were transplanted into C57BL/6J recipient mice (WT or B6.126-Ptger2^{tm1Brey}/J) on day 0. At 21 days after transplantation, mice were treated with (i) saline, (ii) recombinant human relaxin-2 at 0.5 mg/kg (Novartis Pharmaceutical) by continuous infusion with an Alzet mini osmotic pump, (iii) 0.2% β-aminopropionitrile (BAPN; Sigma-Aldrich) in drinking water, (iv) combination of recombinant human relaxin-2 at 0.5 mg/kg and 0.2% BAPN, or (5) combination of recombinant human relaxin-2 at 0.5 mg/kg with anti-LOXL2 antibody at 0.5 mg/kg (Santa Cruz Biotechnology) injected daily intraperitoneally on days 21–35. E prostanoid 2 (EP_2) selective antagonist PF-04418948 (Cayman Chemical) was injected intraperitoneally daily at 10 mg/kg starting 21 days after transplant, with or without relaxin and BAPN. Tracheas were harvested after 14 days of treatment.

Cell culture

Fibroblasts from normal (line CCL-151; ATCC, Manassas, VA) and fibrotic (line CCL-134; ATCC) human lungs were cultured in Dulbecco's modified Eagle medium (DMEM/F-12; Lonza) supplemented with 10% fetal bovine serum, 100 U/mL penicillin, and 100 μg/mL streptomycin. Fibroblasts at passages 2–5, cultured to <80% confluency, were seeded (4647 cells/cm^2) on collagen I–coated polyacrylamide gels (Matrigen) with elastic moduli ranging from 0.5 to 25 kPa. Cells were treated with 1.2 mg/mL recombinant human relaxin-2 with or without PF-04418948 at 10 μM in DMEM/F-12 for 20 h after 4 h of serum starvation.

Immunofluorescent, picrosirius red, and Masson's trichrome staining

Cells were fixed with 4% paraformaldehyde, permeabilized with 0.1% Triton X-100 in phosphate-buffered saline (PBS) supplemented with 1% bovine serum albumin, and immunostained after blocking. Mouse tracheal tissues were fixed with 10% formalin, embedded in paraffin, then cut cross-sectionally with a microtome (Leica Microsystems). The 8-μm tracheal cross-sections were stained by immunofluorescent, picrosirius red, or Masson's trichrome staining. The following primary antibodies were used: phospho–myosin light chain (pMLC) mAb (Cell Signaling Technology), pro–collagen type I mAb, cyclooxygenase 2 (COX2) mAb, leucine-rich repeat–containing G protein-coupled receptor 7/relaxin receptor 1 (LGR7/RXFP1) polyclonal Ab (antibody; Abcam), and conjugated (Cy3) α-SMA mAb (Sigma-Aldrich) at 1:200 dilution. For *in vitro* experiments, collagen production was assessed by expression of procollagen I, a precursor of collagen; fibroblast-to-myofibroblast differentiation was assessed by α-SMA expression. The contraction of myofibroblasts was evaluated and measured by immunofluorescent staining of pMLC and traction force microscopy. Expressions of relaxin receptor on myofibroblasts were evaluated by immunofluorescent staining of RXFP1. Corrected total cell fluorescence (CTCF) was measured by ImageJ (National Institutes of Health) and defined as follows: CTCF = integrated density of selected cell−(area of selected cell × mean fluorescence of background readings). Antirabbit Alexa Fluor 488, antirabbit Cy3, and antirat Cy3 were used for secondary antibodies (Invitrogen).

Hydroxyproline assay

Mice tracheas were weighed, homogenized, and hydrolyzed in hydrochloric acid (12N). Hydroxyproline concentrations were measured according to the manufacturer's instructions (BioVision).

Immunosorbent assays and immunoblot analysis

For immunosorbent assays, supernatants were collected and PGE_2 concentrations were detected by enzyme-linked immunosorbent assay, according to the manufacturer's instructions (Cayman Chemical). For immunoblot analysis, cells were rinsed with PBS and lysed with radioimmunoprecipitation assay buffer supplemented with Halt protease and phosphatase inhibitor cocktail stabilized in dimethylsulfoxide (Thermo Fisher Scientific). Cell lysates were loaded onto SDS-polyacrylamide gels followed by electrophoresis and immunoblot analysis using chemiluminescent immunodetection.

Traction force microscopy

Traction generated by individual cells was measured as described previously (16). Cells were plated at 2 cells/mm^2 on collagen-coated polyacrylamide gels embedded with fluorescent beads (0.5 μm). At 24 hours later, a phase-contrast image and an image of the fluorescent beads immediately underneath the cell were taken. The cells were detached from the gels, and a second image of the same fluorescent beads was taken. Displacement maps and traction fields were obtained by cross-correlating these images.

Statistical analysis

The Shapiro–Wilk test was performed to test whether the data were normally distributed. Statistical significance ($p < 0.05$) was assessed using the unpaired t-test assuming unequal variances between the treatment and saline-control groups for hydroxyproline analysis (Prism Software). A one-way analysis of variance test was used for the multiple group comparisons shown in Figure 5. For histologic analysis, at least 10 tissue sections from each animal (3–20 animals per group) were examined and analyzed with the Mann–Whitney test. Analysis of collagen density in trichrome-stained sections was measured by the ratio of the blue area to the area between the subepithelium and cartilage with ImageJ. For *in vitro* studies, results are from at least three independent experiments, and statistical significance ($p < 0.05$) was assessed using the Mann–Whitney test.

Results

Combined treatment with relaxin and LOX inhibition attenuates established airway fibrosis

Previous studies showed that monotherapy with relaxin or LOX inhibition is effective in preventing fibrosis in animal models (7,8). We assessed whether these drugs could reverse the airway fibrosis in OTT recipients. Non-immunosuppressed allograft OTT mice were treated at 21 days after transplantation, a time point at which fibrosis is well established (Figure S1). These mice were treated with relaxin, BAPN, LOXL2, relaxin with BAPN, relaxin with LOXL2, or saline for 14 days (Figure 1A). Relaxin monotherapy minimally decreased subepithelial collagen deposition, whereas BAPN monotherapy had no effect; however, combined relaxin and BAPN treatment significantly diminished collagen deposition in the subepithelial layer, as demonstrated by histology and hydroxyproline concentration (Figures 1B–D). Moreover, combined treatment with relaxin and BAPN promoted tracheal re-epithelialization with taller cuboidal and pseudostratified epithelium compared with animals in other groups, which exhibited flattened epithelium (Figures 1B and E). Substitution of BAPN with less toxic LOXL2 antibody in combined therapy modestly decreased subepithelial collagen. There was a trend toward decreased hydroxyproline concentration, but this did not meet statistical significance ($p = 0.0542$) (Figure S2).

Decrease in cellular contractility with relaxin is dependent on the type of fibroblast and matrix stiffness

The *in vivo* data indicated that relaxin in combination with LOX inhibition significantly decreased collagen deposition, suggesting that the effectiveness of relaxin may be dependent on ECM stiffness. Prior studies isolated the role of matrix stiffness in cellular functions by plating cells on inert cross-linked polyacrylamide hydrogels (17). The effect of LOX inhibition in our study was modeled *in vitro* by varying the stiffnesses of these matrices. This *in vitro* model was used as a surrogate for BAPN because polyacrylamide gels allow one to isolate the contribution of matrix stiffness, whereas a collagen matrix is limited by the fact that plated cells can migrate into the matrix, changing the stiffness. In addition, it should be noted that because BAPN inhibits collagen cross-linking, it has no action on a polyacrylamide gel.

One measure of stiffness is Young's elastic modulus, which is defined as the force per unit area (in pascals) required to deform a given material. Shkumatov et al measured the stiffness of intrapulmonary airways in the mouse lung by atomic force microscopy and found that the elastic moduli range from 2 to 45 kPa, with a median of 18.6 kPa (18). In another study, Booth et al found that the mean Young's modulus of normal human lungs was 2 kPa, whereas that of tissue from idiopathic pulmonary fibrotic lungs was 16 kPa (19). Consequently, we used 0.5- and 4-kPa matrices to mimic low lung tissue stiffness and 12- and 25-kPa matrices to mimic intermediate to high lung tissue stiffness.

On soft matrices (0.5 and 4 kPa), there was no detectable expression of procollagen I, α-SMA, or pMLC in normal lung fibroblasts (Figures S3 and 2A). On stiff matrices (12 and 25 kPa), the expressions of procollagen I (Figure S3), α-SMA, and pMLC (Figure 2A) were all significantly increased. Relaxin inhibited expression of these markers in normal lung fibroblasts plated on matrices with intermediate stiffness (12 kPa) but not in cells plated on the highest stiffness matrices (25 kPa) (Figure 2A).

Lung fibroblasts from stiff conditions (i.e. fibrotic lung) have been shown to be more contractile than those from normal lungs (20). Consequently, we assessed whether relaxin would regulate the contraction of fibrotic lung fibroblasts and normal lung fibroblasts differently. We found that fibrotic lung fibroblasts were more contractile even with a relatively low matrix stiffness of 4 kPa (Figure 2B). At 4 kPa, relaxin was able to decrease the expression of pMLC (Figure 2B). In contrast, on matrices with intermediate and high stiffness, relaxin failed to reduce pMLC expression. Immunoblots showed that in normal lung fibroblasts, treatment with relaxin significantly decreased pMLC expression at 12 kPa (Figure 2C), but in fibrotic lung fibroblasts, relaxin decreased pMLC expression only at 4 kPa (Figure 2D).

To further examine relaxin's effects on cell contraction, we quantified the contractility of fibrotic and normal lung fibroblasts by traction force microscopy (16). We found

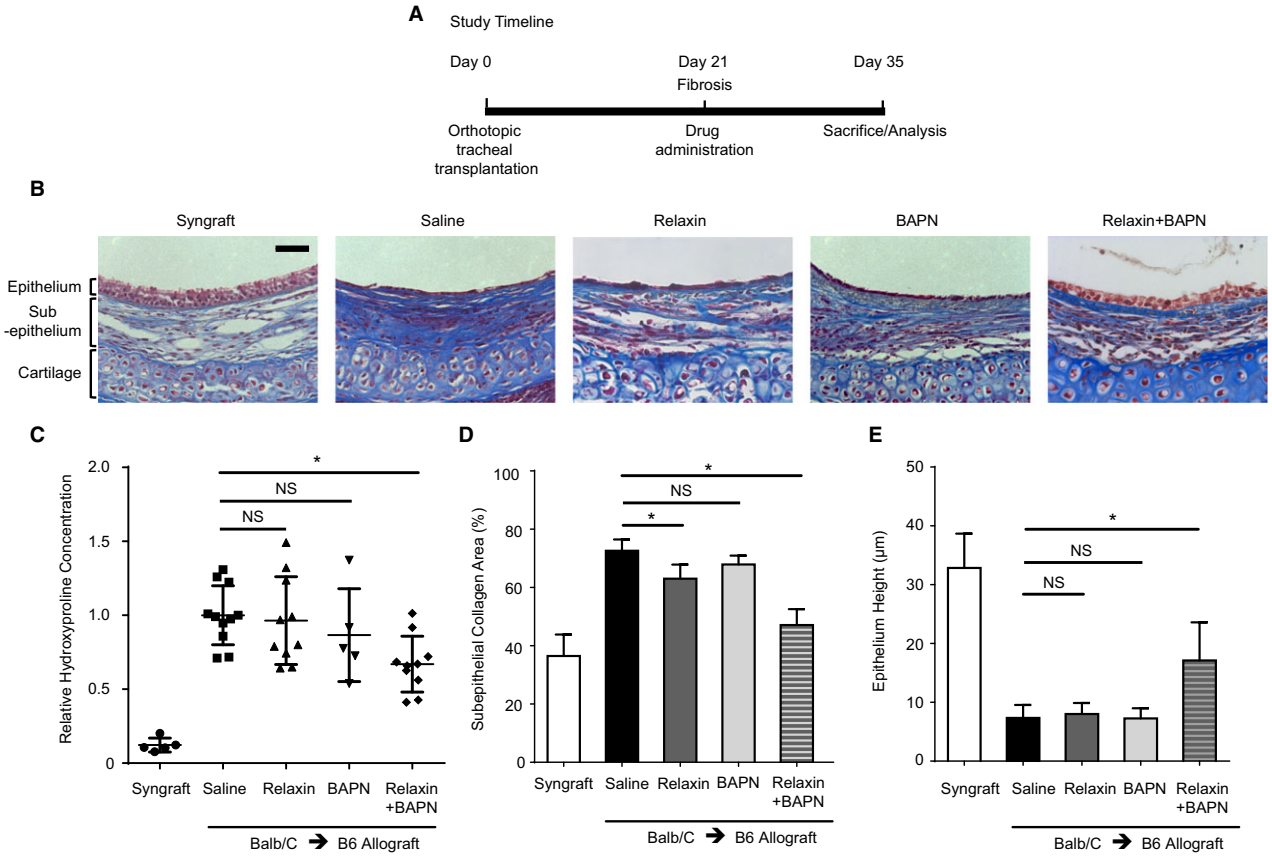

Figure 1: Combined treatment with relaxin and lysyl oxidase (LOX) inhibition attenuates established fibrosis in the orthotopic tracheal transplantation (OTT) model. Tracheal segments from donor mice were transplanted orthotopically into MHC-matched (syngraft) or mismatched (allograft) recipient mice on day 0. (A) Nonimmunosuppressed OTT mice were subjected to treatment at day 21, when fibrosis is well established, for 14 days. Mice were treated with recombinant human relaxin-2 or saline, with or without the LOX inhibitor 0.2% β-aminopropionitrile (BAPN). (B) Representative images of Masson's trichrome staining of tracheal cross-sections in which collagen was stained in blue. Scale bar = 50 μm. (C) Hydroxyproline concentration in tracheal hydrolysates relative to controls was measured to assess the amount of collagen; mean plus or minus standard deviation. (D) Analysis of collagen density in trichrome stained sections measured by the ratio of the blue area to the area between the subepithelium and cartilage with ImageJ; mean plus or minus standard error of the mean (SEM). (E) Measurement of epithelial thickness in tracheal cross-sections from different groups; mean ± SEM. *$p < 0.05$. For (B), (D), and (E), n = 3–10 per group with at least 10 tissue sections per animal. NS, not significant.

that both normal and fibrotic lung fibroblasts exhibited increased contractions with increasing substrate stiffness as measured by root mean square tractions (RMSTs) (Figure 3). Treatment with relaxin decreased the contraction of normal lung fibroblasts plated on 12-kPa matrices but had no significant effects on cells plated on matrices with more stiffness (Figures 3A and C). Treatment with relaxin decreased the contraction of fibrotic lung fibroblasts plated on 4-kPa matrices but had no effects on cells plated on matrices with elastic moduli of ≥12 kPa (Figures 3B and D).

Expression of RXFP1 on fibroblasts is modulated in response to increases in matrix stiffness

Tan et al found that RXFP1 is significantly decreased in the lungs of idiopathic pulmonary fibrosis (IPF) patients and suggested that progression of IPF may be associated with sequential decreases of RXFP1 expression (21). In our study, because relaxin's positive effects were dampened by a stiff microenvironment *in vitro*, we speculated that the expression of RXFP1 would be modulated by a progressive increase in ECM stiffness. We found that expression levels of RXFP1 were significantly higher on fibroblasts plated on soft matrices (0.5 and 4 kPa) than those on fibroblasts cultured on intermediate and stiff matrices (12 and 25 kPa) (Figures 4A and C). Interestingly, cells that expressed higher levels of α-SMA had lower RXFP1 expression (Figure 4A) than cells expressing lower or nondetectable levels of α-SMA. Fibrotic lung fibroblasts had much lower expression of RXFP1 than normal lung fibroblasts. Expression levels of RXFP1 were significantly decreased on fibrotic lung fibroblasts plated

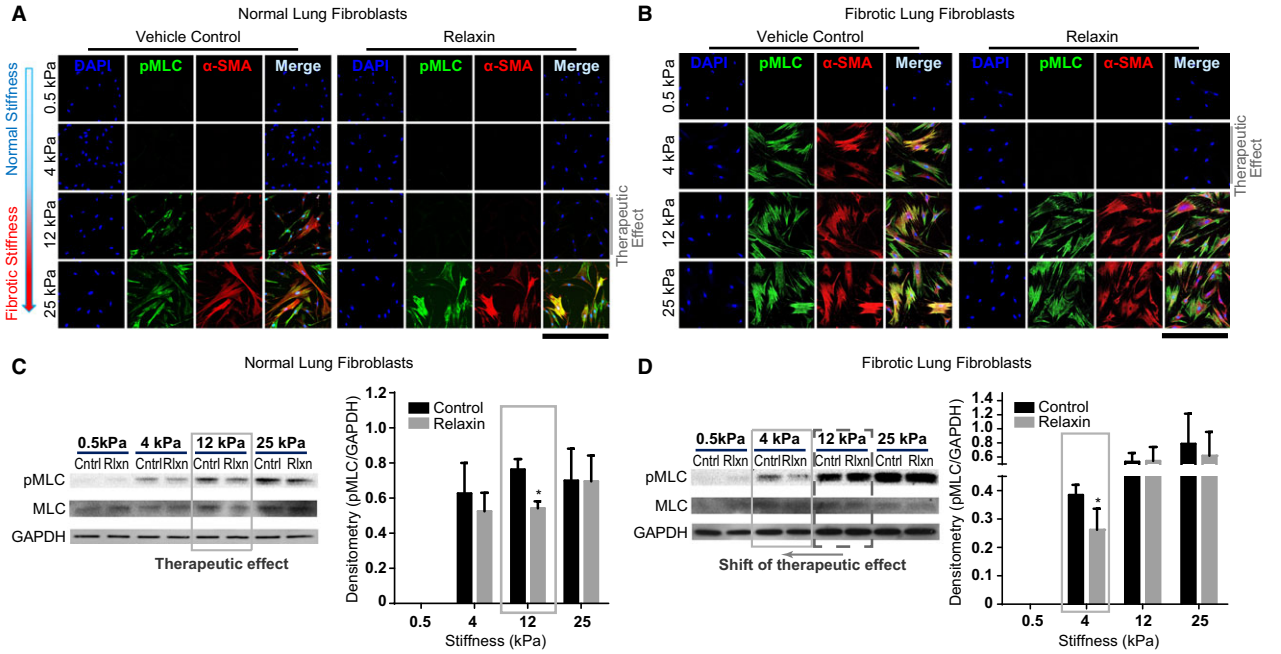

Figure 2: Decrease in cellular contractility with relaxin is dependent on the type of fibroblast and matrix stiffness. Immunofluorescent staining and immunoblot analysis of normal and fibrotic lung fibroblasts. All results are from at least three independent experiments. (A and B) Immunofluorescent staining of normal (A) and fibrotic (B) lung fibroblasts cultured on matrices with Young's elastic moduli of 0.5–25 kPa with and without relaxin. The contraction of cells was evaluated by expression of phospho–myosin light chain (pMLC). Fibroblast-to-myofibroblast differentiation was assessed by α–smooth muscle actin (α-SMA) expression; scale bar = 424 μm. (C and D) Immunoblot analysis of normal (C) and fibrotic (D) lung fibroblasts cultured on matrices with different elastic moduli. Cells were treated without (Cntrl) or with relaxin (Rlxn). The graph represents quantification of the immunoblots by densitometry. Mean plus or minus standard error of the mean. *$p < 0.05$. DAPI, 4′,6-diamidino-2-phenylindole.

on matrices with elastic moduli of ≥4 kPa (Figures 4B and D).

Combined relaxin and LOX inhibition efficacy is dependent on COX2/PGE_2

Next, to address how relaxin may augment LOX inhibition, we evaluated PGE_2, a key eicosanoid implicated in lung fibrosis regulation. PGE_2 is generated when COX2 catalyzes the oxidation of arachidonic acid, and it is the predominant prostaglandin in the lung (22–24). PGE_2 has been shown to decrease cell contractility, and levels of COX2/PGE_2 are significantly decreased in lung fibroblasts (22,25). This led us to investigate whether the effectiveness of combined relaxin and BAPN therapy was mediated through the COX2/PGE_2 pathway.

Mouse tracheal allografts of saline control, relaxin monotherapy, and BAPN monotherapy groups had negligible levels of COX2 expression (Figure 5A). By distinction, tracheas from mice treated with both relaxin and BAPN demonstrated levels of COX2 expression in the epithelium and subepithelium similar to that of tissue from syngrafts. Next, we assessed the expression of COX2 in normal lung fibroblasts on substrates with elastic moduli ranging from 0.5 to 25 kPa. Cells plated on stiff matrices had less COX2 expression than those plated on soft matrices, verifying previous observations (1). Relaxin increased COX2 content in cells from 0.5- and 4-kPa matrices but not from 12- or 25-kPa matrices (Figure 5B). Supernatants of fibroblasts plated on matrices of physiological stiffness (0.5, 1, and 2 kPa) had higher concentrations of PGE_2 than those of cells plated on stiffer matrices (4, 12, and 25 kPa). Relaxin increased PGE_2 levels on all but the stiffest matrices (25 kPa) (Figure 5C).

PGE_2 can ligate four distinct G protein–coupled receptors, termed EP receptors 1–4. Numerous reports have implicated EP_2 as the major receptor mediating inhibitory effects on indices of fibroblast activation (26,27). To confirm that relaxin mediates a decrease in cell contraction by upregulating COX2/PGE_2 production and signaling via the EP_2 receptor, we inhibited the actions of PGE_2 by treating normal lung fibroblasts with PF-04418948, a potent and selective EP_2 antagonist. This EP_2 antagonist prevented the relaxin-mediated reduction of pMLC and α-SMA in cells cultured on the 12-kPa matrices (Figure 6A).

To test whether the beneficial effects of the combined treatment of relaxin and BAPN *in vivo* could be

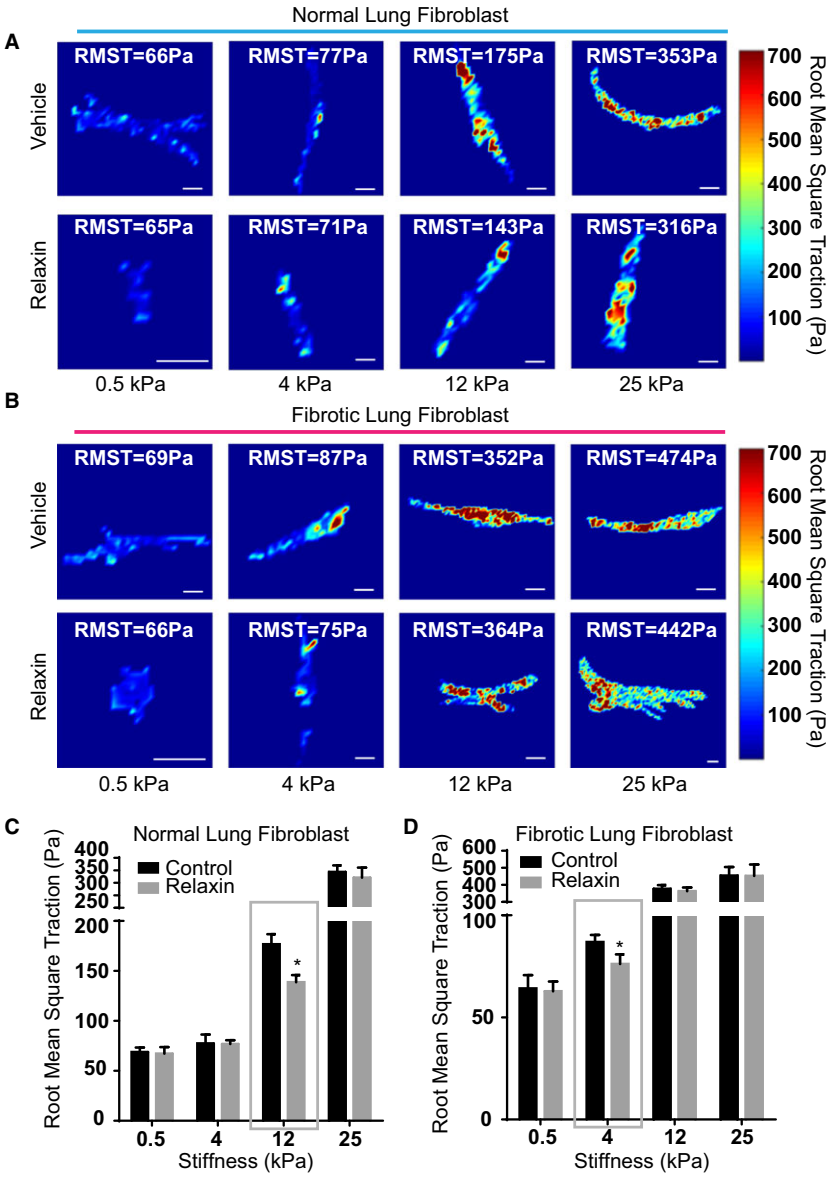

Figure 3: Root mean square tractions (RMSTs) of cells measured by traction force microscopy. (A and B) Representative traction fields (in pascals) of normal (A) and fibrotic (B) lung fibroblasts plated on matrices with Young's elastic moduli 0.5–25 kPa. (C and D) Analysis of RMSTs of normal (C) and fibrotic (D) lung fibroblasts plated on matrices with different elastic moduli. Mean plus or minus standard error of the mean. n = 8–15 per group, scale bars = 20 μm, *$p < 0.05$.

abrogated by inhibition of the COX2/PGE2/EP_2 pathway, OTT mice at 21 days after transplantation were treated with saline, PF-04418948, or combined relaxin and BAPN treatment with or without PF-04418948. Furthermore, OTT EP_2 receptor KO mice (B6.126-Ptger2^{tm1Brey}/J) were treated with or without the combination of relaxin and BAPN. Suppression of PGE_2 signaling with the EP_2 receptor antagonist in the combined treatment group abrogated the protective effect of combined treatment, with specimens exhibiting dense deposition of subepithelial collagen and no restoration of cuboidal epithelium (Figures 6B and C). Similarly, treatment with relaxin and BAPN lost its beneficial effects in EP_2 KO mice. Tracheas from PF-04418948–treated mice and EP_2 KO mice had higher amounts of collagen than those from saline-treated control mice, as shown in hydroxyproline concentration measurement. Combined treatment of relaxin and BAPN failed to decrease collagen amount in tracheas from PF-04418948–treated WT and EP_2 KO mice (Figures 6C and D), providing further support that relaxin and BAPN act through the COX2/PGE_2/EP_2 pathway.

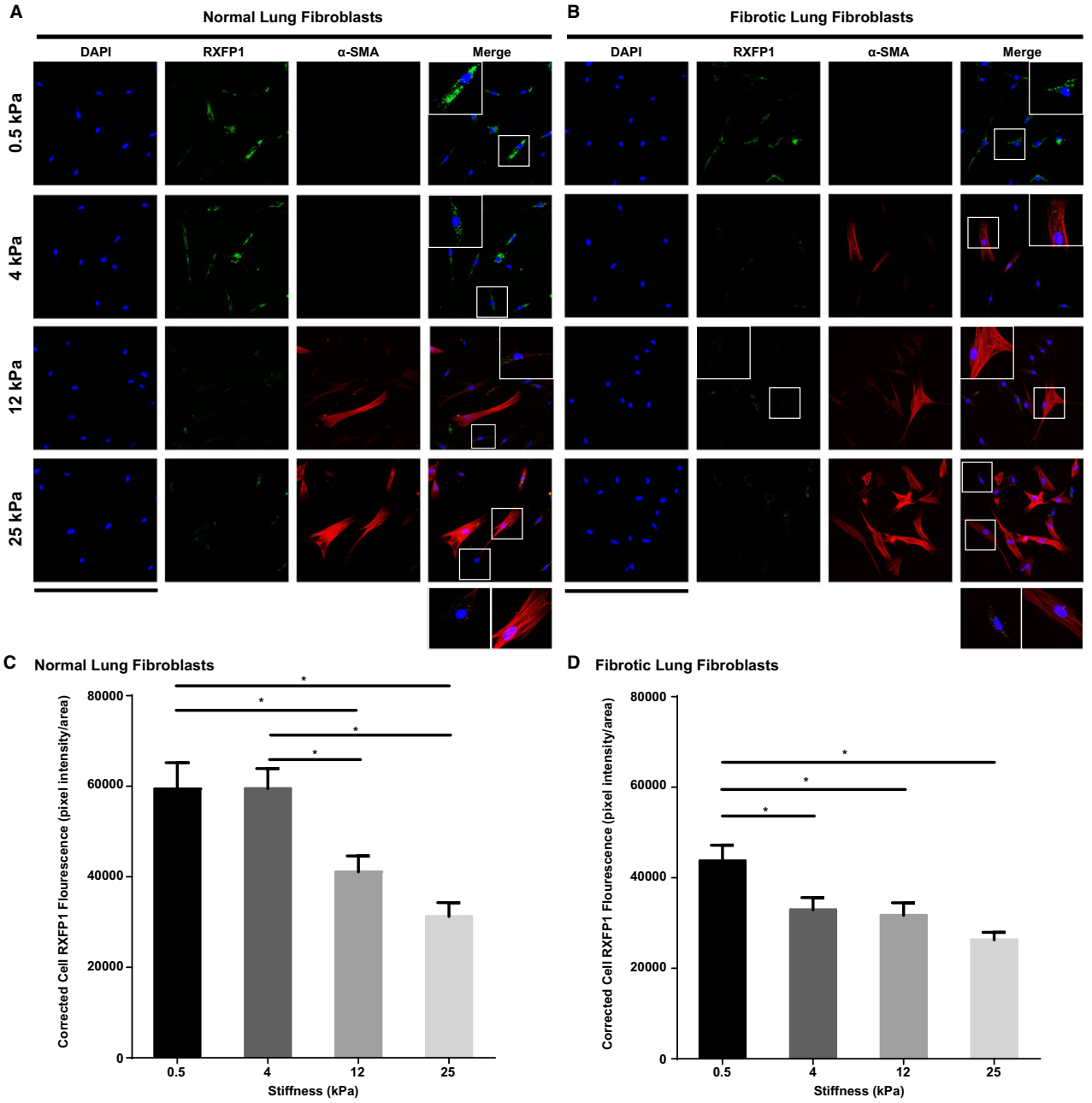

Figure 4: Expression of relaxin receptor 1 (RXFP1) on fibroblasts. (A and B) Immunofluorescent staining of RXFP1 on normal (A) and fibrotic (B) lung fibroblasts cultured on matrices with Young's elastic moduli of 0.5–25 kPa. Fibroblast-to-myofibroblast differentiation was assessed by α-smooth muscle actin (α-SMA) expression; scale bar = 424 μm; inserts are ×4 magnification of selected area. (C and D) Corrected total cell fluorescence of normal (C) and fibrotic (D) lung fibroblasts cultured on matrices with different elastic moduli (measured by ImageJ). Mean plus or minus standard error of the mean. n = 40–50 per group, *$p < 0.05$. DAPI, 4′,6-diamidino-2-phenylindole.

Discussion

Preclinical studies have used a large number of therapies that have demonstrated the reversal of fibrosis in animal models; however, very few have been found to be effective in human fibrotic diseases. The discrepancy between the preclinical and clinical findings may be result in part from the use of models of fibrosis that are not robust. Compared with other fibrotic models such as the bleomycin-injured lung model, which is

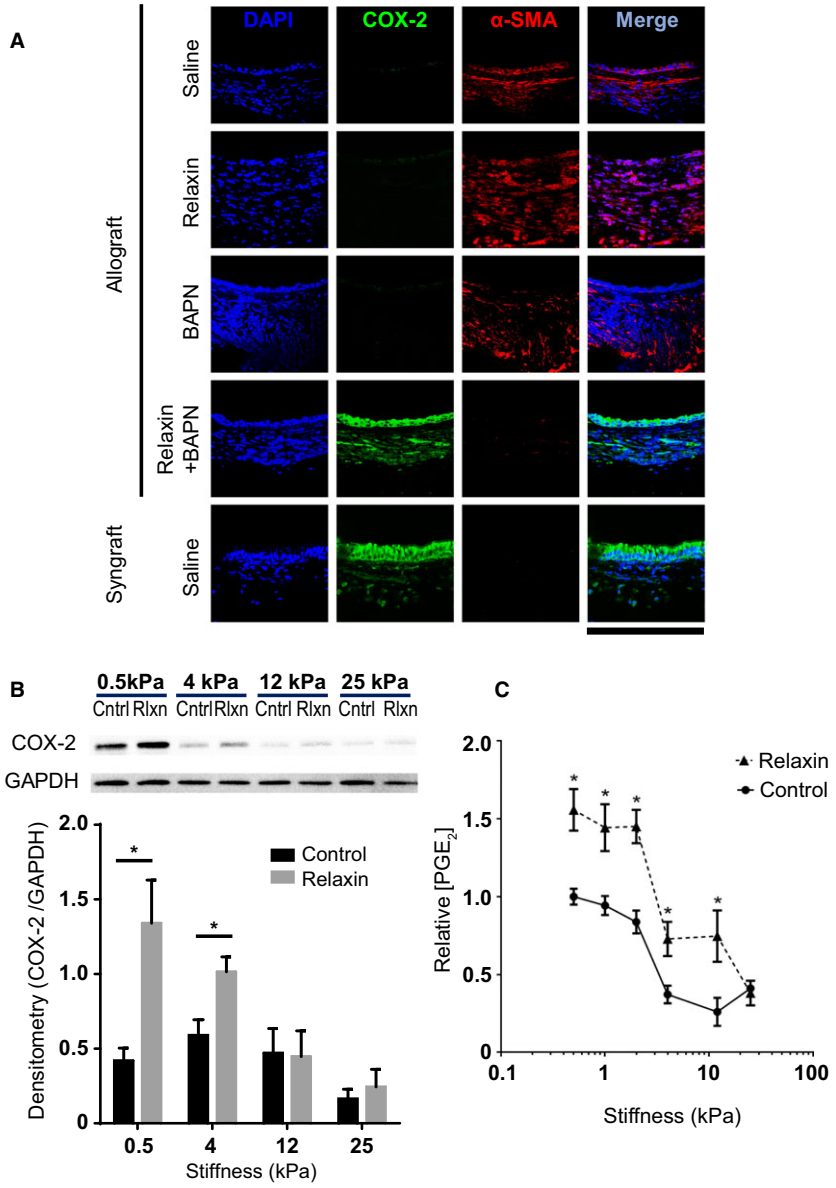

Figure 5: Relaxin induces cyclooxygenase 2 (COX2) and prostaglandin E_2 (PGE_2) in a stiffness-dependent manner. (A) Immunofluorescent staining of tracheal cross-sections; scale bar = 212 μm; n = 3–10 per group with at least 10 tissue sections per animal. (B) Immunoblots of normal lung fibroblast lysates. Cells were plated on matrices with different elastic moduli and were treated without (Cntrl) and with relaxin (Rlxn); results were from at least three independent experiments. The graph represents quantification of the immunoblot by densitometry; mean plus or minus standard error of the mean (SEM). (C) Normal human lung fibroblasts were cultured on matrices with Young's elastic moduli of 0.5, 1, 2, 4, 12, and 25 kPa and treated with or without relaxin. Supernatants of cells were collected, and PGE_2 concentrations were detected by PGE_2 enzyme-linked immunosorbent assay; mean ± SEM. n = 5–10 per group. *$p < 0.05$. BAPN, β-aminopropionitrile; DAPI, 4′,6-diamidino-2-phenylindole.

spontaneously reversible, tissue remodeling in the OTT model is particularly robust and progressive, driven by inflammation (alloimmunity) not present in nontransplant models of fibrosis. Treatment of the OTT model with numerous immunosuppressant and antifibrotic agents, including high-dose steroids, anti-CD40L, anti–lymphocyte function-associated antigen 1 (anti-LFA1), combined anti-CD40L/anti-LFA1 (14), and pirfenidone, have not been able to reverse fibrosis (data not shown). In this study, we demonstrated that combined therapy with relaxin and LOX inhibition reversed established airway fibrosis by targeting both intracellular and extracellular biophysical properties of the graft—cellular contractility and ECM stiffness—and in this manner appeared to promote

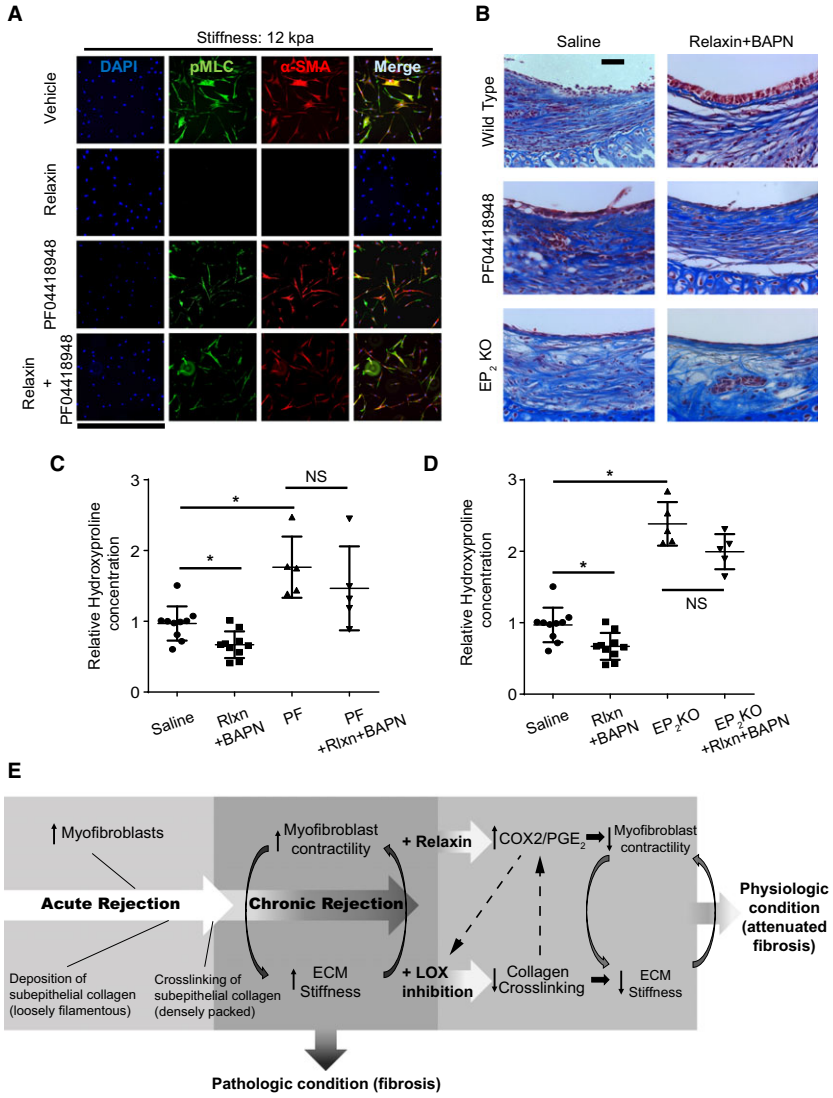

Figure 6: Prostaglandin E_2 (PGE_2) inhibition abrogates the beneficial effects of relaxin and β-aminopropionitrile (BAPN) combined treatment. (A) Immunofluorescent staining of lung fibroblasts cultured on matrices with Young's elastic moduli of 12 kPa. Cells were treated with Dulbecco's modified Eagle medium only, relaxin, PF-04418948 (E prostanoid 2 [EP_2] antagonist), or PF-04418948 with relaxin. Results are from at least three independent experiments; scale bar = 848 μm. (B) Representative images of Masson's trichrome staining of tracheal cross-sections; scale bar = 50 μm; n = 3–10 per group with at least 10 tissue sections per animal. (C and D) Hydroxyproline concentration in tracheal hydrolysates relative to controls was measured to assess the amount of collagen. Mean plus or minus standard deviation. *$p < 0.05$, Tukey's test was used as a post hoc test. (E) At the end of acute rejection, there is infiltration of myofibroblasts that deposit collagen. Cross-linking of loose collagen is catalyzed by lysyl oxidase (LOX) to form densely packed fibers that increase extracellular matrix (ECM) stiffness. Fibrotic ECM stiffness may then activate cells to be more contractile, leading to further collagen deposition. This positive feedback loop leads to persistent fibrosis and creates a pathological condition. Relaxin upregulates cyclooxygenase 2 (COX2) and prostaglandin E_2 (PGE_2), decreasing cellular contraction, which in turn promotes ECM softening. LOX inhibition downregulates collagen cross-linking, thereby decreasing ECM stiffness, which in turn decreases myofibroblast contractility. This breaks the positive feedback loop and returns the tissue to a physiological condition. Furthermore, $COX2/PGE_2$ may contribute to further decrease collagen cross-linking and ECM softening through LOX inhibition. A soft ECM may also increase $COX2/PGE_2$, which in turn can decrease myofibroblast contractility. These mechanisms may further support the reversal of fibrosis. α-SMA, α–smooth muscle actin; BAPN, β-aminopropionitrile; ECM, extracellular matrix; NS, not significant; PF, PF-04418948; pMLC, phospho–myosin light chain; Rlxn, relaxin.

the conversion toward a normal, nonremodeled, epithelialized airway.

As described, myofibroblast activation and contraction contribute to ECM stiffening and further fibrotic progression. Myofibroblast contractility is regulated by MLC phosphorylation, which enables myosin to interact with actin filaments to generate force. We found that pMLC and RMST of lung fibroblasts cultured on matrices with soft and intermediate stiffness were downregulated by relaxin. Relaxin also decreased α-SMA and procollagen I expression in normal lung fibroblasts on matrices with soft or intermediate stiffness but lost its effects on very stiff matrices. In the mouse OTT model, monotherapy with relaxin had only a minimal effect in reversing fibrosis. Given the *in vitro* findings, we suspect that relaxin alone was not effective in reversing fibrosis in the OTT model (and possible fibrosis in human) because the ECM of the tracheas was already very stiff.

Relaxin was first named for its ability to relax the female reproductive tract during pregnancy (28). It is produced by both sexes and has been shown to act intracellularly to induce cellular relaxation and to ameliorate fibrosis (29). Relaxin and its G protein–coupled receptors are found in rodent and human lungs, predominantly within bronchial epithelial cells, fibroblasts, and airway smooth muscle cells (6,30). Intriguingly, relaxin-deficient mice develop age-associated fibrosis in the lung and skin (31,32). However, as stated earlier, phase II and III trials of relaxin did not demonstrate any efficacy in the treatment of fibrosis in systemic sclerosis (8). It has been shown that RXFP1 level is decreased in lungs of IPF patients (21). We found that fibroblasts that were plated on stiff matrices had significantly lower RXFP1 expression than those plated on soft matrices. This may suggest that expression of RXFP1 is associated with progressive increase of ECM stiffness in fibrosis. Consequently, we speculate that the lack of effect in established dermal fibrosis may be due to the relatively high tissue stiffness.

Tissue stiffening results mainly from the cross-linking of ECM proteins (33). LOX converts collagen from soluble monomers to insoluble fibers by oxidizing peptidyl lysine to form covalent cross-linkages, thereby increasing ECM stiffness (9). Inhibition of LOX with BAPN decreased α-SMA expression and fibrotic tissue stiffness in a carbon tetrachloride–induced liver fibrosis model. (11). In a bleomycin lung model, inhibition of LOXL2 with a monoclonal antibody decreased collagen deposition (12). Nevertheless, a clinical phase II trial was terminated because of lack of efficacy. Intriguingly, the current study modeled persistent alloimmune injury, and LOX inhibitor monotherapy failed to reverse established fibrosis. We modeled the effect of LOX inhibition and isolated the role of substrate stiffness by plating cells on inert polyacrylamide gels with stiffnesses ranging from normal to fibrotic tissues. We found that soft (0.5 and 4 kPa) but not intermediate or stiff (12 and 25 kPa) substrates prevented expression of procollagen I and the differentiation and contraction of fibroblasts. These findings suggest that the chronically rejected trachea is stiffer than normal airways (range 2–45 kPa (18)) and exceeded the threshold below which the profibrotic feedback loop could be interrupted by LOX inhibition alone.

Fibrotic lungs express less COX-2/PGE_2 than healthy lungs (34). We found that allogeneic transplanted tracheas have less COX2 and more α-SMA expression than syngeneic transplants. Allografts from mice treated with combined relaxin/LOX inhibition express more COX2 than those from monotherapies. *In vitro*, relaxin upregulated COX2 expression and PGE_2 secretion in fibroblasts cultured on soft matrices but not on stiff matrices. Relaxin boosted the secretion of endogenous PGE_2 from cells on low- to intermediate-stiffness matrices but failed to increase PGE_2 levels in cells cultured on pathologically stiff matrices (≥25 kPa). These results suggest that relaxin's ability to upregulate COX2/PGE_2 is dampened by a stiff microenvironment. This was also observed in previous studies that demonstrated that a stiff ECM suppresses the secretion of COX2/PGE_2. Previous investigations showed that PGE_2 signaling through the EP_2 receptor inhibits lung myofibroblast differentiation, contraction, and secretion of collagen (26,35). We found that treatment with an EP_2 receptor antagonist abrogated the effects of relaxin on cells cultured in the intermediate-stiffness matrices and the beneficial effects of combined treatment on fibrotic airways. These results cumulatively indicate that the effectiveness of combined relaxin and BAPN treatment in abrogating subepithelial fibrosis is mediated through COX2 expression, PGE_2 biosynthesis, and EP_2 signaling.

In addition to decreasing myofibroblast contractility directly, PGE_2 has also been shown to inhibit LOX (36), which may contribute to further decrease in collagen cross-linking and softening of the ECM. Moreover, Liu et al demonstrated that a stiff ECM suppresses the COX2/PGE_2 pathway (1); therefore, decreasing collagen cross-linking with LOX inhibition may lead to increased COX2/PGE_2, which in turn can decrease myofibroblast contractility. These mechanisms may further support the reversal of fibrosis (Figure 6E).

Combined treatment not only decreased subepithelial fibrosis but also promoted an epithelium expressing a high level of COX2. Konoeda et al showed that fibrosis in the chronically rejected airways is associated with an aberrant flattened epithelium, and the damage to epithelial cells appears before subepithelial fibrosis (37). In contrast to the flattened epithelium observed in other treatment groups, mice treated with combined therapy had taller, more cuboidal, and occasionally

pseudostratified epithelial layers. Because the airway epithelium is a major source of PGE_2 (38), its damage could lead to decreased levels of PGE_2 in the airway and an inability to inhibit fibroblast proliferation and activation, thereby promoting subepithelial fibrosis. However, the mechanism by which combined therapy with relaxin and LOX inhibition contribute to the development of this columnar epithelium requires further investigation. Prior studies showed that PGE_2 deficiency in lung fibrosis leads to increased airway epithelial cell apoptosis, and PGE_2 has been shown to promote epithelial cell proliferation and migration (39,40). We speculate that the collagen-rich subepithelium is unable to support a pseudostratified columnar epithelium, perhaps in part because of a deficiency of COX2/PGE_2.

A limitation of this study is that we were unable to confirm that LOX inhibition decreased tracheal stiffness *in vivo*. We attempted to measure the elastic moduli of the tracheas with atomic-force microscopy but found wide variability within each sample, with point-to–point differences up to 10 kPa (data not shown). Previous studies have shown that Young's elastic moduli of non-cartilaginous lung airways range from 2 to 45 kPa (18). We suspect that the variability in cartilaginous airways will be even higher. Another limitation of this study is that although BAPN is a potent irreversible inhibitor of LOX, wider clinical use is limited by its side effects, such as osteolethyrism, a disorder that can lead to skeletal deformations (41). We replaced BAPN with nontoxic LOXL2 antibody and found that the combined treatment of relaxin and LOXL2 had a less significant effect on reduction of collagen. BAPN was used in this study as a proof of concept; for clinical use, other less toxic and more potent LOX or LOX-like inhibitors in conjunction with relaxin could be tested.

In summary, we demonstrated reversal of transplanted airway fibrosis by targeting both intracellular and extracellular biophysical properties of the allograft. We showed that relaxin increases the expression of COX2/PGE_2 and thus decreases cellular contraction, whereas LOX inhibition decreases tissue stiffness; together, they may shift the airway toward a physiological state (Figure 6E). The reversal of established fibrosis achieved in this work may represent a novel therapeutic strategy for the treatment of chronic rejection in solid organ transplantation and other fibrotic diseases.

Acknowledgments

We thank Dr. Daniel Tschumperlin and Dr. Norbert Voelkel for their critical reviews of the manuscript. We also thank Dr. Dennis Stewart and Novartis Pharmaceuticals for their assistance and generosity in supplying rh-relaxin-2. This work was funded by National Heart, Lung and Blood Institute, National Institute of Health, grants 1P01HL10879701 and RO1HL095686.

Author Contributions

Y.C. Lin and M.R. Nicolls designed research; Y.C. Lin analyzed data and performed research; Y.C. Lin, Y.K. Song, X. Jiang, M. Peters-Golden, and M.R. Nicolls wrote the paper; M. Peters-Golden contributed research materials.

Disclosure

The authors of this manuscript have no conflicts of interest to disclose as described by the *American Journal of Transplantation*.

References

1. Liu F, Mih JD, Shea BS, et al. Feedback amplification of fibrosis through matrix stiffening and COX-2 suppression. J Cell Biol 2010; 190: 693–706.
2. Klingberg F, Hinz B, White ES. The myofibroblast matrix: Implications for tissue repair and fibrosis. J Pathol 2013; 229: 298–309.
3. Wipff P-J, Rifkin DB, Meister J-J, Hinz B. Myofibroblast contraction activates latent TGF-beta 1 from the extracellular matrix. J Cell Biol 2007; 179: 1311–1323.
4. Zhou Y, Huang XW, Hecker L, et al. Inhibition of mechanosensitive signaling in myofibroblasts ameliorates experimental pulmonary fibrosis. J Clin Invest 2013; 123: 1096–1108.
5. Huang X, Gai Y, Yang N, et al. Relaxin regulates myofibroblast contractility and protects against lung fibrosis. Am J Pathol 2011; 179: 2751–2765.
6. Royce SG, Miao YR, Lee M, Samuel CS, Tregear GW, Tang MLK. Relaxin reverses airway remodeling and airway dysfunction in allergic airways disease. Endocrinology 2009; 150: 2692–2699.
7. Seibold JR, Korn JH, Simms R, et al. Recombinant human relaxin in the treatment of scleroderma - A randomized, double-blind, placebo-controlled trial. Ann Intern Med 2000; 132: 871–879.
8. Seibold JR. Relaxins: Lessons and limitations. Curr Rheumatol Rep 2002; 4: 275–276.
9. Lucero HA, Kagan HM. Lysyl oxidase: An oxidative enzyme and effector of cell function. Cell Mol Life Sci 2006; 63: 2304–2316.
10. Lopez B, Gonzalez A, Hermida N, Valencia F, de Teresa E, Diez J. Role of lysyl oxidase in myocardial fibrosis: From basic science to clinical aspects. Am J Physiol Heart Circ Physiol 2010; 299: H1–H9.
11. Georges PC, Hui J-J, Gombos Z, et al. Increased stiffness of the rat liver precedes matrix deposition: Implications for fibrosis. Am J Physiol Gastrointest Liver Physiol 2007; 293: G1147–G1154.
12. Barry-Hamilton V, Spangler R, Marshall D, et al. Allosteric inhibition of lysyl oxidase-like-2 impedes the development of a pathologic microenvironment. Nat Med 2010; 16: 1009–1017.
13. Genden EM, Boros P, Liu JH, Bromberg JS, Mayer L. Orthotopic tracheal transplantation in the murine model. Transplantation 2002; 73: 1420–1425.
14. Babu AN, Murakawa T, Thurman JM, et al. Microvascular destruction identifies murine allografts that cannot be rescued from airway fibrosis. J Clin Invest 2007; 117: 3774–3785.

15. Jiang X, Khan MA, Tian W, et al. Adenovirus-mediated HIF-1 alpha gene transfer promotes repair of mouse airway allograft microvasculature and attenuates chronic rejection. J Clin Invest 2011; 121: 2336–2349.
16. Butler JP, Tolic-Norrelykke IM, Fabry B, Fredberg JJ. Traction fields, moments, and strain energy that cells exert on their surroundings. Am J Physiol Cell Physiol 2002; 282: C595–C605.
17. Pelham RJ, Wang YL. Cell locomotion and focal adhesions are regulated by substrate flexibility. Proc Natl Acad Sci USA 1997; 94: 13661–13665.
18. Shkumatov A, Thompson M, Choi KM, et al. Matrix stiffness-modulated proliferation and secretory function of the airway smooth muscle cells. Am J Physiol Lung Cell Mol Physiol 2015; 308: L1125–L1135.
19. Booth AJ, Hadley R, Cornett AM, et al. Acellular Normal and Fibrotic Human Lung Matrices as a Culture System for *In Vitro* Investigation. Am J Respir Crit Care Med 2012; 186: 866–876.
20. Hinz B. Mechanical aspects of lung fibrosis: A spotlight on the myofibroblast. Proc Am Thorac Soc 2012; 9: 137–147.
21. Tan J, Tedrow JR, Dutta JA, et al. Expression of RXFP1 is decreased in idiopathic pulmonary fibrosis: Implications for relaxin-based therapies. Am J Respir Crit Care Med 2016;. doi:10.1164/rccm.201509-1865OC.
22. Wilborn J, Crofford LJ, Burdick MD, Kunkel SL, Strieter RM, Petersgolden M. Cultured lung fibroblasts isolated from patients with idiopathic pulmonary fibrosis have a diminished capacity to synthesize prostaglandin E(2), and to express cyclooxygenase-2. J Clin Invest 1995; 95: 1861–1868.
23. Huang SK, Peters-Golden M. Eicosanoid lipid mediators in fibrotic lung diseases: Ready for prime time? Chest 2008; 133: 1442–1450.
24. Ozaki T, Rennard SI, Crystal RG. Cyclooxygenase metabolites are compartmentalized in the human lower respiratory-tract. J Appl Physiol 1987; 62: 219–222.
25. Borok Z, Gillissen A, Buhl R, et al. Augmentation of functional prostaglandin-E levels on the respiratory epithelial surface by aerosol administration of prostaglandin-E. Am Rev Respir Dis 1991; 144: 1080–1084.
26. Kolodsick JE, Peters-Golden M, Larios J, Toews GB, Thannickal VJ, Moore BB. Prostaglandin E-2 inhibits fibroblast to myofibroblast transition via E. prostanoid receptor 2 signaling and cyclic adenosine monophosphate elevation. Am J Respir Cell Mol Biol 2003; 29: 537–544.
27. Huang S, Wettlaufer SH, Hogaboam C, Aronoff DM, Peters-Golden M. Prostaglandin E-2 inhibits collagen expression and proliferation in patient-derived normal lung fibroblasts via E prostanoid 2 receptor and cAMP signaling. Am J Physiol Lung Cell Mol Physiol 2007; 292: L405–L413.
28. Hisaw FL. Experimental relaxation of the pubic ligament of the guinea pig. Proc Soc Exp Biol Med 1926; 23: 661–663.
29. Bennett RG. Relaxin and its role in the development and treatment of fibrosis. Transl Res 2009; 154: 1–6.
30. Hsu SY, Nakabayashi K, Nishi S, et al. Activation of orphan receptors by the hormone relaxin. Science 2002; 295: 671–674.
31. Samuel CS, Zhao C, Bathgate RAD, et al. Relaxin deficiency in mice is associated with an age-related progression of pulmonary fibrosis. FASEB J 2003; 17: 121–123.
32. Samuel CS, Royce SG, Chen B, et al. Relaxin family peptide receptor-1 protects against airway fibrosis during homeostasis but not against fibrosis associated with chronic allergic airways disease. Endocrinology 2009; 150: 1495–1502.
33. Parker MW, Rossi D, Peterson M, et al. Fibrotic extracellular matrix activates a profibrotic positive feedback loop. J Clin Invest 2014; 124: 1622–1635.
34. Huang SK, White ES, Wettlaufer SH, et al. Prostaglandin E-2 induces fibroblast apoptosis by modulating multiple survival pathways. FASEB J 2009; 23: 4317–4326.
35. Garrison G, Huang SK, Okunishi K, et al. Reversal of myofibroblast differentiation by prostaglandin E-2. Am J Respir Cell Mol Biol 2013; 48: 550–558.
36. Boak AM, Roy R, Berk J, et al. Regulation of lysyl oxidase expression in lung fibroblasts by transforming growth factor-beta(1) and prostaglandin E(2). Am J Respir Cell Mol Biol 1994; 11: 751–755.
37. Konoeda C, Koinuma D, Morishita Y, et al. Epithelial to mesenchymal transition in murine tracheal allotransplantation: An immunohistochemical observation. Transplant Proc 2013; 45: 1797–1801.
38. Lama V, Moore BB, Christensen P, Toews GB, Peters-Golden M. Prostaglandin E-2 synthesis and suppression of fibroblast proliferation by alveolar epithelial cells is cyclooxygenase-2-dependent. Am J Respir Cell Mol Biol 2002; 27: 752–758.
39. Maher TM, Evans IC, Bottoms SE, et al. Diminished prostaglandin E-2 contributes to the apoptosis paradox in idiopathic pulmonary fibrosis. Am J Respir Crit Care Med 2010; 182: 73–82.
40. Savla U, Appel HJ, Sporn PHS, Waters CM. Prostaglandin E-2 regulates wound closure in airway epithelium. Am J Physiol Lung Cell Mol Physiol 2001; 280: L421–L431.
41. Dawson DA, Rinaldi AC, Poch G. Biochemical and toxicological evaluation of agent-cofactor reactivity as a mechanism of action for osteolathyrism. Toxicology 2002; 177: 267–284.

Supporting Information

Additional Supporting Information may be found in the online version of this article.

Figure S1. Airway fibrosis is established at day 21 after transplantation. (A, B) Representative images of picrosirius red staining of tracheal cross-sections at days 21 and 35 after transplantation. Under bright field microscopy, collagen is stained red. Under polarized light, large and dense collagen bundles are visualized in orange and yellow. (C) In tracheal sections from relaxin and β-aminopropionitrile (BAPN)–treated mice, under polarized light, thin and loose collagen fibers are visualized in green. Scale bar = 50 μm.

Figure S2. Combined treatment with relaxin and lysyl oxidase–like 2 (LOXL2) inhibition attenuates established fibrosis in orthotopic tracheal transplantation (OTT) tracheas. (A) Representative images of Masson's trichrome staining of tracheal cross-sections in which collagen was stained in blue. Scale bar = 50 μm; n = 3–10 per group with at least 10 tissue sections per animal. (B) Analysis of collagen density in trichrome-stained sections measured by the ratio of the blue area to the area between the subepithelium and cartilage; mean plus or minus standard error of the mean; *$p < 0.05$. (C) Hydroxyproline concentration in tracheal hydrolysates relative to

controls was measured to assess the amount of collagen. Mean plus or minus standard deviation; p = 0.054.

Figure S3. Immunofluorescent staining of human normal lung fibroblasts cultured with and without relaxin on matrices with Young's elastic moduli of 0.5, 4, 12, and 25 kPa. Collagen production was assessed by expression of procollagen I; fibroblast-to-myofibroblast differentiation was assessed by α–smooth muscle actin (α-SMA) expression. Results are from at least three independent experiments; scale bar = 848 μm.